(2)

FRACTURE MECHANICS ANALYSIS FOR SHORT CRACKS

B. S. Annigeri

R90-957565-F

FINAL REPORT

February 1990

Prepared for

Air Force Office of Scientific Research
Bolling AFB, Washington, DC 20332

Contract F49620-86-C-0095

UNITED
TECHNOLOGIES
RESEARCH
CENTER
East Hartford, Connecticut 06108

(a)

SECURITY CLASSIFICATION OF THIS PAGE

REPORT DOCUMENTATION PAGE

Form Approved OMB No. 0704-0188

1a. REPORT SECURITY CLASSIFICATION: unclassified	1b. RESTRICTIVE MARKINGS
2a. SECURITY CLASSIFICATION AUTHORITY	3. DISTRIBUTION/AVAILABILITY OF REPORT: Approved for public release, distribution unlimited
2b. DECLASSIFICATION/DOWNGRADING SCHEDULE	
4. PERFORMING ORGANIZATION REPORT NUMBER(S): R90-957565-F	5. MONITORING ORGANIZATION REPORT NUMBER(S): AFOSR-TR- 90-0545
6a. NAME OF PERFORMING ORGANIZATION: United Technologies Res. Ctr. (6b. OFFICE SYMBOL (If applicable))	7a. NAME OF MONITORING ORGANIZATION: AFOSR
6c. ADDRESS (City, State, and ZIP Code): 400 Main St. East Hartford, CT 06108	7b. ADDRESS (City, State, and ZIP Code): Det 5, Pratt & Whitney Aircraft Group 400 Main St. East Hartford, CT 06108
8a. NAME OF FUNDING/SPONSORING ORGANIZATION: AFSOR/NA USAF/AFSC Directorate of Aero. Sciences (8b. OFFICE SYMBOL (If applicable): NA)	9. PROCUREMENT INSTRUMENT IDENTIFICATION NUMBER: F49620-86-C-0095
8c. ADDRESS (City, State, and ZIP Code): Bldg. 410, Bolling Air Force Base, Washington, DC 20332	10. SOURCE OF FUNDING NUMBERS: PROGRAM ELEMENT NO. 61102F; PROJECT NO. 2302; TASK NO. B2; WORK UNIT ACCESSION NO.
11. TITLE (Include Security Classification): "Fracture Mechanics Analysis for Short Cracks (a)	
12. PERSONAL AUTHOR(S): B. S. Annigeri	
13a. TYPE OF REPORT: Final Report (13b. TIME COVERED FROM Aug 86 TO Dec 90)	14. DATE OF REPORT (Year, Month, Day): 1990 February 27 (15. PAGE COUNT: 37)
16. SUPPLEMENTARY NOTATION	
17. COSATI CODES: FIELD / GROUP / SUB-GROUP	18. SUBJECT TERMS (Continue on reverse if necessary and identify by block number): Fracture, Finite Element, Fatigue, JES, Short Cracks, Integral Equation,

19. ABSTRACT (Continue on reverse if necessary and identify by block number)

This report pertains to the development of the Surface Integral and Finite Element (SAFE) hybrid method for the analysis of short or physically small cracks. The development of yield strip models for modeling crack tip plasticity is presented. The effects of loading and unloading are investigated with regard to plastic zone size and residual deformation. Calculations for the opening loads are presented for long and short cracks and the difference in fatigue crack growth behavior is determined and correlated to the effective stress intensity factor range.

20. DISTRIBUTION/AVAILABILITY OF ABSTRACT: ☐ UNCLASSIFIED/UNLIMITED ☑ SAME AS RPT. ☑ DTIC USERS	21. ABSTRACT SECURITY CLASSIFICATION: unclassified
22a. NAME OF RESPONSIBLE INDIVIDUAL: Lt. Col. George K. Haritos	22b. TELEPHONE (Include Area Code): (202) 767-4935 (22c. OFFICE SYMBOL: NA)

DD Form 1473, JUN 86 Previous editions are obsolete. SECURITY CLASSIFICATION OF THIS PAGE unclassified

90 05 21 104

SUMMARY

This is the final technical report pertaining to the further development of the Surface-Integral and Finite Element hybrid method for the analysis of short or phsyically small cracks. The central objective of this research has been to develop a predictive capability for determining the differences in the crack driving force for *short* and *long* cracks.

The yielding of material at the crack tip and the subsequent propagation of the crack due to fatigue loading leaves a wake of material that has been plastically deformed. This wake controls the amount of crack closure and affects long and short cracks differently. The crack closure has been shown to be greater for long cracks; thus, short cracks can experience a greater crack tip driving force resulting in a faster propagation rate. To model the plastic yielding, the Surface-Integral and Finite Element Hybrid Method is further developed for crack tip plasticity by the use of yield strip models. Dugdale and Bilby-Cottrell-Swinden (BCS) type yield strip models have been implemented in the hybrid code. These model capture the dominant effects of plasticity near the crack tip and provide an efficient procedure for computing the crack tip opening and slip displacement for short (and long) cracks. Results obtained for a center crack panel problem under tensile and shear loading using the hybrid method are in excellent agreement with analytical solutions. The differences in closure for long and short cracks has been determined by computation of the effective stress intensity factor range.

This final report covers the period between August 1, 1986 to December 31, 1989. The work reported herein was under the sponsorship of the AFOSR under the technical direction of Lt. Col. G. K. Haritos.

R90-957565-F

Fracture Mechanics Analysis for Short Cracks

TABLE OF CONTENTS

1.0 INTRODUCTION

Materials that are used for the manufacture of structural components inherently contain flaws or defects such as inclusions, voids, porosities, microcracks, etc. The presence of a flaw thus has to be accounted for in the design of structural components. These flaws can grow, especially under fatigue loading, and it is important to be able to predict the evolution of these flaws as a function of the loading. Fracture mechanics has been developed and applied successfully for the analysis of cracks and associated crack propagation. The Griffith–Irwin–Orowan linear elastic fracture mechanics (LEFM) theory has been adequate for modeling cracks in structural components where the elastic K (Stress Intensity Factor) fields dominate the solution (Refs. 1 and 2). The K dominance is appropriate when the plastic zone size is small compared to the length of the crack and other dimensions of the body. The development of LEFM has been followed by the development of elastic–plastic fracture mechanics (EPFM) with the pioneering works of Hult and McClintock (Ref. 3), Dugdale (Ref. 4), Barenblatt (Ref. 5), Bilby, Cottrell and Swinden (Refs. 6 and 7), Rice (Ref. 8), and Hutchinson (Ref. 9). EPFM is applicable and needed especially for high toughness and low strength materials where the elastic K dominance may not be satisfied and has to be replaced by evaluating the energy release rate, for example, by using the J integral. The J integral is based on the existence of a strain energy functional and is strictly valid for a crack under monotonic loading.

An important mode of crack propagation in structural components is due to fatigue which can occur under constant or variable amplitude loading; a typical crack growth curve is shown in Fig. 1. This crack growth behavior can be broken into three regions. Region 1 corresponds to slow crack growth, Region 2 corresponds to steady state growth, and Region 3 represents rapid unstable crack growth. The steady state crack growth can be represented by the Paris – Erdogan power law relation given below:

$$\frac{da}{dN} = C\ (\Delta K)^m \qquad (1)$$

where, a = the crack length; N = the number of fatigue cycles; ΔK = the stress intensity factor (SIF) range; C and m are material parameters.

It has been well documented in the literature (Refs. 10–14) that short or physically small cracks can grow faster than long cracks (refer to Fig. 2). Typically, this behavior can occur at stress intensity

factor ranges lower than the stress intensity factor threshold based on long crack data. Thus in structural components which have dominant small (or short) cracks distributed in the microstructure,the use of long crack data could lead to underestimates of crack growth rate or overestimates of fatigue life. One of the primary reasons for this behavior of short cracks is crack closure (Ref. 10). The closure is due to the evolution of plastic deformation at the crack tip and along the crack faces. At the crack tip, the linear elastic fracture mechanics (LEFM) asymptotic solution for the stress tensor is as given below:

$$\sigma_{ij} = \frac{K_\alpha}{\sqrt{2\pi r}} g_{ij}(\theta) \tag{2}$$

where, σ_{ij} is the stress tensor; K_α = the stress intensity factor for mode α ; r = the radial distance from the crack tip; g_{ij} = function of angular location θ, θ = angular location of the radius vector at the crack tip. The extent of the monotonic plastic zone at the crack tip is shown in Fig. 3. The size r_p of the plastic zone is approximately given by (these are obtained using the asymptotic elastic solution):

$$r_p = \frac{1}{\pi}\left(\frac{K_\alpha}{\sigma_y}\right)^2 \text{ (for plane stress)} \tag{3}$$

$$r_p = \frac{1}{3\pi}\left(\frac{K_\alpha}{\sigma_y}\right)^2 \text{ (for plane strain)} \tag{4}$$

where K_α represents the Mode I, Mode II or Mode III stress intensity factor.

The plastic zone sizes under repeated or fatigue loadings are however different than their monotonic counterparts. An estimate of the plastic zone can be made based on the theory of proportional plastic flow i.e., the components of the plastic strain tensor remain in constant proportion at every point in the plastic region. Hult and McClintock (Ref. 3) and Rice (Ref. 24) have developed a plastic superposition method for Mode II shear loading and Mode I tensile loading respectively. The plastic zone for Mode I loading is shown in Fig. 4 (Ref. 24). This zone is quarter the size of the corresponding monotonic plastic zone. This estimate will be less accurate if deviations from proportional

loading exist such as due to the formation of shear bands and other hardening mechanisms. The size of the plastic zone with reverse unloading is then given by:

$$r_p = \frac{1}{\pi}\left(\frac{K_a}{2\sigma_y}\right)^2 \text{(for plane stress)} \tag{5}$$

$$r_p = \frac{1}{3\pi}\left(\frac{K_a}{2\sigma_y}\right)^2 \text{(for plane strain)} \tag{6}$$

The fatigue crack growth is a result of damage accumulating in the process zone, which is contained within the plastic zone. Here deformation results in the formation of slip bands, microcracks and their coalescence resulting in macrocracks. The direction of propagation can initiate in the slip plane direction and then change to an average normal to the maximum principle tensile stress direction (Ref. 30). There are two modes of crack growth: transcrystalline (across the crystal) and intercrystalline (along the grain boundaries). These various modes depend on the temperature, grain size, etc. In any event whether the crack is a physically small or short crack or a long crack, a plastically deformed zone (wake) is always left behind. The plastic wake causes closure of the crack surfaces, and its effect on short and long cracks is different thus causing changes in the crack driving force acting at the crack tip. These changes can lead to short cracks growing faster or at a lower threshold than long cracks; and, hence it is important to predict this behavior. The plasticity at the crack tip can cause the crack tip to close even though the loading is tension–tension. This means that the crack can close earlier and open later than the monotonic values of SIF based on LEFM. The value of the stress intensity factor at closing and opening are labeled as K_{op} and K_{cl} (Fig. 5). Typically K_{op} and K_{cl} are very close within the scatter band of experimental data and can be assumed to be identical for practical purposes (Ref. 16). The stress intensity factor range then is given by:

$$\Delta K = K_{max} - K_{op} \tag{7}$$

This range can then be used in a fatigue equation such as the Paris Erdogan type power law for prediction of fatigue crack growth.

Crack closure can also be caused by oxide induced and roughness induced phenomena. The oxide induced closure is due to the oxidation of freshly exposed surfaces which can wedge between the crack surfaces. Roughness induced closure is due to the nature of the fracture morphology and can be a result of Mode II shear displacement (Ref. 12). In this report, the effect of plasticity induced closure is considered and the development of the Surface Integral and Finite Element Hybrid method for plasticity is presented.

2.0 DEFINITIONS OF VARIOUS TYPES OF SHORT CRACKS

Short cracks have been defined in a number of ways. The definitions given below are from Ref. 10.

(1) Cracks which are of a length comparable to the size of the microstructure, e.g. of the order of the grain size.

(2) Cracks which are of a length comparable to the scale of local plasticity, typically $\leq 10^{-2}$ mm in ultrahigh strength materials and $\leq 0.1 - 1$ mm in low strength materials.

(3) Cracks which are physically small $\leq 0.5 - 1$ mm.

In this research effort, the second and third definitions will be used for defining short cracks. Also since a two dimensional analysis is being utilized, the crack can be long in the thickness direction. For the first type of crack, anisotropy of the grain will be important; for the ones defined by (2) and (3) elastic-plastic fracture mechanics will be necessary as the elastic K fields may not dominate at the crack tip.

3.0 FORMULATION OF THE SURFACE INTEGRAL AND FINITE ELEMENT (SAFE) HYBRID METHOD FOR FRACTURE MECHANICS

The Surface Integral and Finite Element Hybrid method is a very effective method that has been developed for modeling evolution of fractures in finite continua. The fractures are modeled using a continuous distribution of dislocations which results in a singular integral formulation. The uncracked body including any nonhomogeneity is modeled using a finite element model. These two models are superposed ensuring appropriate traction and displacement matching on the boundaries. A thesis (Ref. 17) and several papers/reports have been written on this subject (Refs. 18–23).

3.1 FORMULATION OF THE SAFE METHOD FOR LINEAR ANALYSIS

The details of the development of the SAFE method are given in Refs. 18–23. The governing equation is derived using linear superposition of the Surface Integral and Finite Element models (Fig. 6) ensuring appropriate traction and displacement matching at the boundaries.

$$\begin{bmatrix} K & G-KL \\ S & C-SL \end{bmatrix} \begin{Bmatrix} U \\ F \end{Bmatrix} = \begin{Bmatrix} R \\ T \end{Bmatrix} \tag{8}$$

where,

K = Finite element stiffness matrix of the uncracked body

C = Coefficient matrix for the singular integral equation

G = Boundary force correction matrix

S = Stress feedback matrix

L = Displacement matrix for the singular integral equation

U = Total displacement vector at the finite element nodes

F = Vector of amplitudes of the dislocation density

R = Vector of applied nodal loads

T = Vector of applied tractions along the crack

In Fig. 6, R^c is the boundary force

$$R^c = [G]\ \{F\} \tag{9}$$

and T^c is the traction along the crack line

$$T^c = [S]\ \{U^{FE}\} \tag{10}$$

The governing equations for the FE and SI models are:

$$[K]\ \{U^{FE}\} = R - R^c \tag{11}$$

and,

$$[C]\{F\} = T - T^c \tag{12}$$

Also, the total displacement field is given by,

$$\{U\} = \{U^{FE}\} + \{U^{SI}\} \tag{13}$$

where,

U^{FE} = Finite element displacements for the plate without the crack

U^{SI} = Surface integral displacements for a crack in an infinite domain

$$\{U^{SI}\} = [L]\{F\} \tag{14}$$

Using Eqs. (9) through (14) results in the coupled governing equation (8) for the SAFE hybrid method.

3.2 FORMULATION OF THE SAFE METHOD FOR MATERIALLY NONLINEAR ANALYSIS

In an earlier report (Ref. 21) a method for modeling nonhomogeneity was presented that used the finite element mesh to correct for plasticity. For modeling the plastic field at the crack tip, especially for short cracks, the need for a fine finite element representation would still be necessary with that method. In order to alleviate this problem the approach taken here is that of modeling plasticity using yield strip models. The development of the Surface Integral and Finite Element Hybrid Method with yield strips is given in the following.

As a first order correction to the LEFM stress intensity factor solutions, Dugdale (Ref. 4) and Barenblatt (Ref. 5) proposed a yield strip model which is valid for plane stress situations and typically useful for thin sheets. An elastic perfectly plastic material model is used in the analysis. The Dugdale model which is for Mode I loading uses yield strips which are additional ligaments at the end of the crack tips. The Bilby, Cottrell and Swinden (BCS) model (Ref. 6) is similar to the Dugdale model but is for in-plane Mode II shear loading. These yield strips can support a maximum stress equal to the yield stress for the material. The basis of implementing the yield strip models in the Surface Integral and Finite Element Hybrid Method can be developed by considering the problem of a crack in a plate as shown in Fig. 7. The physical length of the crack is 2a; appended to the crack tips are two yield strips whose length is c. These yield strips can sustain a maximum stress corresponding to the yield stress in tension for the opening (Mode I) case or the yield stress in shear for the shear (Mode II) case. This problem can be expressed as the sum of a finite domain without a crack and an infinite domain with a crack, using incremental linear superposition. The finite domain without the crack is modeled effectively using the finite element method; the infinite domain with the crack(s) is modeled effectively using the surface integral method which is based on dislocation theory. Since the crack is being modeled in an infinite plate, an appropriate boundary load correction vector R^c is computed using the surface integral model and applied to the finite element model to ensure that the correct load is applied to the boundary. Similarly, the traction vector T^c in the uncracked body which is acting along the original crack location is computed using the finite element model and applied to the surface integral model. The traction vector T_y is assembled using the yield stress values in tension and shear for the material. Note that the traction applied along the yield strips is $T_y - T^c$.

The governing equation for the hybrid method with yield strips is obtained as follows. The finite element equation for the uncracked plate is given by:

$$[K]\left[U^{FE}\right] = \{R\} - \{R^c\} \tag{15}$$

[K] = finite element stiffness matrix of the uncracked body; $\{U^{FE}\}$ = vector of unknown finite element nodal displacements for the uncracked body; $\{R\}$ = vector of applied loads; $\{R^c\}$ = load correction for the boundary due to the presence of the crack.

The crack in an infinite domain is represented by using a continuous distribution of dislocations leading to a singular integral equation formulation (Ref. 18). The integral equation for an infinite domain with .. crack is given by:

$$\vec{T}(x_0) = \vec{n} \cdot \int_{S_c} \Gamma(\vec{x}, \vec{x_0}) \cdot \mu(\vec{x})\, dS_c \tag{16}$$

$T(x_0)$ = traction at x_0 due to a distribution of dislocations along the crack surface; $\vec{n}$ = the normal to the crack surface at x_0; $\Gamma(\vec{x}, \vec{x_0})$ = fundamental stress solution for a dislocation (kernel function); $\mu(\vec{x})$ = dislocation density at $\vec{x}$; S_c = surface area of the crack. The singular integral equation is evaluated numerically in the Cauchy principal value sense and the discretized form of Eq. (16) is:

$$[C]\{F\} = \{T\} - \{T^c\} + \{T_y\} \tag{17}$$

[C] = coefficient matrix for the singular integral equation; {F} = vector of amplitudes of the dislocation density (for two dimensional analysis); {T} = vector of applied tractions along the crack; $\{T^c\}$ = traction vector for the crack surfaces due to the applied load $R - R^c$ on the finite element model. $\{T_y\}$ = traction vector assembled using the yield stress values for the material and applied to the yield strips.

Equations (15) and (17) are fully coupled through the boundary force correction matrix G ($R^c = [G]\{F\}$) and the stress feedback matrix S ($T^c = [S]\{U^{FE}\}$) which leads to the following representation for the hybrid formulation:

$$\begin{bmatrix} K & G \\ S & C \end{bmatrix} \begin{Bmatrix} U^{FE} \\ F \end{Bmatrix} = \begin{Bmatrix} R \\ T + T_y \end{Bmatrix} \tag{18}$$

In Eq. (18), the variable U^{FE} represents the continuous displacement field due to just the finite element model. This has to be changed to the total displacement field by addition of the discontinuous field due to the crack so that the displacement boundary conditions can be enforced, as follows:

$$\{U\} = \{U^{FE}\} + \{U^{SI}\} \tag{19}$$

$\{U^{SI}\}$ = vector of unknown finite element nodal displacements due to the surface integral model. $\{U^{SI}\}$ is obtained by setting up the integral equation for displacements and evaluating the integral (Annigeri and Cleary (Ref. 18)).

$$\{U^{SI}\} = [L]\{F\} \tag{20}$$

[L] = displacement matrix. Thus, Eqs. (18), (19), and (20) can be combined to form the governing equation for the hybrid formulation:

$$\begin{bmatrix} K & G - KL \\ S & C - SL \end{bmatrix} \begin{Bmatrix} U \\ F \end{Bmatrix} = \begin{Bmatrix} R \\ T + T_y \end{Bmatrix} \tag{21}$$

Equation (21) allows imposition of arbitrary force, traction and displacement boundary conditions. The sparsity and symmetry of the stiffness matrix is taken full advantage of using a special solution scheme which has been reported in Annigeri and Cleary (Ref. 19). As is evident, the basic problem of a crack with yield strips is a nonlinear one as the length of the yield strips is dependent on the applied loading. A modified Newton algorithm with interval halving (Ref. 31) has been implemented in the SAFE Hybrid computer code for determining the length of the yield strips. The length of the yield strip is changed until K_I and/or K_{II} is reduced to a small value within a certain tolerance. This algorithm has worked very effectively in being able to compute the length of the yield strip. Results are presented in the next section.

3.3 RESULTS

3.3.1 Plate with a Center Crack – Mode I (Pure Tension – Dugdale Model). A plate with a center crack loaded with a uniform tensile load is shown in Fig. 10. The dimensions of the plate and other material parameters are also given in the figure. Plane stress condition and an elastic perfectly plastic model (Fig. 8) is used to determine the constitutive behavior. The yield strip length and the crack tip opening displacement (CTOD) for the center crack problem in an infinite medium can be obtained using the Dugdale solution (Ref. 4) (refer to Fig. 9). The solution obtained using the SAFE hybrid code is given in Figs. 11 and 12. The SAFE results are in excellent agreement with the Dugdale solutions. The departure of SAFE predictions for a half crack length of greater than 0.3 is due to the Dugdale solution being valid only for the infinite domain.

3.3.2 Plate with a Center Crack – Mode II (Pure Shear – Bilby–Cottrell–Swinden Model). A plate with a center crack loaded with a pure shear loading is shown in Fig. 13. The SAFE results are given in Figs. 14 and 15. Again, the SAFE results for yield strip length and the crack tip slip development (CTSD) compare very well with the analytical solutions of Bilby, Cottrell and Swinden (Ref. 6).

For plane strain conditions, inclined strip models at the crack tip can be used to determine the extent of the plastic zone and the CTOD and CTSD (Ref. 25–28).

3.3.3 Monotonic Loading and Unloading under a Tensile Load. Budiansky and Hutchinson (BH) (Ref. 29) have presented a remarkable paper on the use of yield strips for the analysis of closure in fatigue. Using the principle of plastic superposition (Refs. 3, 24, 29) the length of the yield zone after unloading can be determined as shown in Figs. 4 and 16. At $K = K_{min} = 0$ the length of the yield zone under compression is one fourth of the yield zone under monotic loading $K = K_{max}$. This result has been verified using the SAFE code for the problem given in Fig. 10. The crack tip opening displacement comparison is given in Table 1. The difference between the BH solution and the SAFE prediction is due to the fact that the BH solution is for CTOD at the crack tip while the SAFE results are at the collocation point just behind the crack tip. The yield strip lengths for both BH and SAFE are in good agreement as shown in the table. The size of the reversed plastic zone is obtained by varying the length over which $-\sigma_y$ is applied so that the singularity at the original crack tip is reduced to small value (Ref. 29).

Table 1 – Results for tensile loading of a center cracked panel.		
σ_y = 30,000 psi	σ = 15,000 psi	
E = .3E8 psi	ν = .3	Crack length = .16 in.
	BH (Ref. 29)	SAFE
Yield strip length	.0662	.063
CTOD (loaded K = K_{max})	1.685E–04	1.59E–04
Size of reversed plastic zone	.0165	.016
CTOD (unloaded K = K_{min} = 0)	.8425E–04	1.038E–04

For a growing crack (as discussed in Ref. 29), the displacement behind the crack tip as obtained by monotonic loading and unloading is not sufficient to include the plastic deformation that occurs and gets attached to the surfaces of the crack. To accommodate this plastic residual deformation, the problem is reposed as shown in Fig. 17. Here residual dislocation $\delta = \delta_R$ is left attached to the crack faces. This is based on the assumption that the crack has been growing from a small size and thus the need for modeling the residual dislocation. BH were dealing with a semi-infinite crack but the same logic has been adopted here for a finite crack in a finite body. What this entails is that the residual dislocation has the same value behind the crack tip(s). Note that the dislocation δ_M comes from the K = K_{max} loading condition. The length of the yield zone (oa) for a growing crack is obtained by using the loading on the crack as shown in Fig. 17 and iterating so that the singularity at the original crack tip is reduced to a small value. The results for the growing crack are given in Table 2. There is good agreement between the BH and the SAFE predictions. The extent of the reversed plastic zone is reduced to about 10 percent of the Dugdale plastic zone for loading. The reversed plastic zone is embedded in the original plastic zone due to loading.

Table 2 – Results for tensile loading of a center cracked panel (growing crack)		
	BH (Ref. 29)	SAFE
Yield strip length	.0662	.064
CTOD (K = K_{max})	1.685E–04	1.59E–04
Size of reversed plastic zone	.0066	.0064
CTOD (K = K_{min} = 0)	1.44E–04	1.434E–04

3.3.4 Determination of K_{op} and Crack Growth for Long and Short Cracks. In the previous section, the calculations for a growing crack that has been unloaded has been performed. In this section the crack will be reloaded and the load required to open the crack will be determined. For fatigue crack

growth, the effective stress intensity factor range which is calculated by the equation shown below is important as it includes the effect of crack closure.

$$\Delta\bar{K}_{eff} = \frac{S_{max} - S_o}{S_{max} - S_{min}} \Delta\bar{K} \qquad (22)$$

where, $\Delta\bar{K}$ is the stress intensity factor range calculated after adjusting the crack length for the yield strip length

$\Delta\bar{K}_{eff}$ = $\Delta\bar{K}$ effective

S_{max} = Maximum applied stress

S_{min} = Minimum applied stress

S_o = Crack opening stress

The reloading of the crack after unloading is done as shown in Fig. 18 with the residual deformation left on the yield strip from the previous unloaded state. Then the load is increased until the crack tip opens beyond the residual stretch δ_R left from the previous state (see Ref. 29 for details).

Newman (Refs. 13 and 14) has developed an analytical closure model for determining the closure and crack opening stresses S_o for a finite body with a growing crack. The contact problem is modeled using rigid perfectly plastic bar elements. In Ref. 14, a table is provided for data on 2024–T3 Alclad aluminum center cracked test (CCT) specimens. This data is shown in Table 3. The dimensions of the CCT specimen are width = 80mm, thickness t = 2mm. The tensile strength (σ_u) and the assumed flow stress (σ_o) of the material is 475 Mpa. The maximum applied stress level S_{max} was 77.5 Mpa at an R ratio of .01. A plot of log da/dn against log ΔK was constructed as shown in Fig. 19. In Table 3, the calculated S_o/S_{max} using Newman's closure model have also been tabulated.

The SAFE prediction of K_{op} for a crack length of .23 cm at a ΔK level of 6.59 MPa $-m^{1/2}$ is 0.56. Since the opening stresses are stabilized after this crack length, the analysis was performed for crack lengths less than .2 cm for simulating short crack behavior. This is shown in Fig. 19 where the SAFE predictions show an increase in the crack growth rate for short cracks. This is due to the value of S_o/S_{max} being less for short cracks as compared with S_o/S_{max} = .56 for a long crack. The da/dN rate for the short crack is determined by interpolating da/dN versus $\Delta\bar{K}_{effective}$ baseline long crack data given in Table 3.

Table 3. da/dN data for 2024–T3 ALCLAD Aluminum Alloy Sheet from Ref. 14 with SAFE results.					
$\frac{da}{dN}$, mm/cycle	ΔK, MPa $-m^{1/2}$	$\Delta \overline{K}$, MPa $-m^{1/2}$	$\frac{S_o}{S_{max}}$	$\Delta \overline{K}_{eff}$, MPa $-m^{1/2}$	SAFE $\frac{S_o}{S_{max}}$
7.6E–06	6.59	6.70	0.571	2.90	.56
3.0E–05	8.79	8.95	.596	3.65	
4.3E–05	12.64	12.86	.597	5.23	
6.8E–05	14.29	14.58	.596	5.95	
1.2E–04	17.58	18.06	.600	7.30	
3.8E–04	19.78	20.20	.599	8.18	
1.3E–03	25.28	25.88	.594	10.61	
7.6E–03	36.27	38.25	.578	16.30	

The results show good agreement between growth rate predictions of short cracks (starting from 1 mm crack size) with the short crack growth data from Ref. 14. In Ref. 14, the data is for growth of short cracks from holes. The SAFE predictions are for a center cracked panel but the comparison is made with data for short cracks emanating from a small hole (R = 2 mm). The radius of the hole being very small does not affect this comparison appreciably but there is some difference as shown in Fig. 19. In the SAFE code, holes, notches can be also easily modeled. The predictions are obtained by using $\overline{\Delta K}_{effective}$ versus da/dN long crack data and interpolating to get results for small cracks. The S_0/S_{max} calculated using SAFE for the short cracks were 0.4, 0.5 and 0.52, respectively for the three points shown in the figure.

3.4 CONCLUSIONS AND FUTURE RESEARCH OBJECTIVES

The Surface Integral and finite Element Hybrid method has been developed for modeling crack tip plasticity using yield strip models. With relatively few degrees of freedom, the hybrid method can predict the crack tip opening and slip displacements very accurately. This has been demonstrated by comparison of the SAFE predictions with the classical solutions of Dugdale and Bilby, Cottrell and Swinden for Mode I and Mode II loading, respectively. The advantage of the hybrid method is that the finite element discretization is not changed for long or short cracks. This is due to the fact that the cracks and associated plasticity are represented by use of dislocations which results in a singular integral equation formulation. The yield strip models developed can be used for plane stress and plane strain. For plane strain conditions, inclined yield strip models have to be used at the crack tip (Refs.

25–28). The SAFE code can also model plane strain conditions but the results presented here are for plane stress.

The SAFE predictions for the plastic zone sizes for loading and unloading are in good agreement with the results of Budiansky and Hutchinson (Ref. 29). For growth of fatigue cracks, it is important to determine the ratio of the opening stress and the maximum stress (S_0/S_{max}). This ratio determines the differences between the crack closure for long cracks and short cracks. SAFE predictions for the opening stresses and crack growth rates compare well with the results of Newman (Refs. 13 and 14).

The yield strip model is effective for modeling contained plasticity and has been shown to be useful for modeling short (small) and long cracks. Future work should focus on predicting crack growth for various R (K_{min}/K_{max}) ratios and also for different materials for plane stress and plane strain conditions. The inclined strip yield model should be further developed for modeling the plastic wake effects under plane strain conditions.

REFERENCES

1. Rolfe, S. T., and Barsom, J.M.: "Fatigue and Fracture Control of Structures" Prentice Hall, 1977.

2. Kanninen, M. F. and Popelar, C. H.: Advanced Fracture Mechanics, Oxford University Press, 1985.

3. Hult, J. A. and McClintock, F. A., "Elastic-Plastic Stress and Strain Distribution Around Sharp Notches Under Repeated Shear," Proceedings of the 9th International Conference for Applied Mechanics, Vol. 8, pp. 51–58, Brussels, 1956.

4. Dugdale, D. S.: "Yielding of Steel Sheets Containing Slits," Journal of the Mechanics and Physics of Solids, Vol. 8, pp. 100–108, 1960.

5. Barenblatt, G. I: "The Mathematical Theory of Equilibirium of a Crack in Brittle Fracture", Avances in Applied Mechanics, Vol. 7, pp. 55–129, 1962.

6. Bilby, B. A., Cottrell, A. H. and Swinden, K. H.: "The Spread of Plastic Yield from a Notch," Proceedings of the Royal Society, Series A, Vol. 272, pp. 304–314, 1963.

7. Bilby, B. A. and Swinden, K. H.: "Representation of Plasticity at Notches by Linear Dislocation Arrays," Proceedings of the Royal Society, A285, pp. 22–33, 1965.

8. Rice, J. R.: Mathematical Analysis in the Mechanics of Fracture, Chapter 3 of Fracture: An Advanced Treatise, Leibowitz H., ed., Vol. 2, pp. 191–311, Academic Press, New York, 1968.

9, Hutchinson, J. W.: "Singular Behavior at the End of a Tensile Crack in a Hardening Material", Journal of the Mechanics and Physics of Solids, Vol. 16, pp. 13–31, 1968.

10. Suresh., S. and Ritchie, R. O.: "Propagation of Short Fatigue Cracks," International Metal Reviews, Vol. 29, No. 6, pp. 445–476, 1983.

11. Dowling, N. E.: "Crack Growth During Low-Cycle Fatigue of Smooth Axial Specimens," ASTM-STP 637, American Society of Testing and Materials, pp. 97–121, 1977.

12. Holm, D. K. and Blom, A. F.: "Short Cracks and Closure in AL2024–T3," The Aeronautical Research Institute of Sweden, Report No. FFA TN 1984 –40, 1984.

13. Newman, J. C., Jr.: A Crack Closure Model for Predicting Fatigue Crack Growth Under Aircraft Spectrum Loading. Methods And Models for Predicting Fatigue Crack Growth under Random Loading, J.B. Chang and C.M. Hudson, eds., ASTM STP 748, pp. 53–84, 1981.

14. Newman, J. C., Jr.: "A Nonlinear Fracture Mechanics Approach to the Growth of Small Cracks," Proc. of the 55th meeting of the AGARD Structural and Materials Panel on Behavior of Short Cracks in Airframe Components, Toronto , Canada, September 1982.

15. Iyyer, N. S. and Dowling, N. E.: "Closure of Fatigue Cracks at High Strains," NASA Contractor Report 175021, December 1985.

16. Banerjee, S.: "A Review of Crack Closure," AFWAL-TR-84-4031, April 1984.

17. Annigeri, B. S.: Surface Integral Finite Element Hybrid Method for Localized Problems in Continuum Mechanics, Sc.D thesis in Dept. of Mechanical Engineering, M.I.T., 1984.

18. Annigeri, B. S. and Cleary, M. P.: "Surface Integral Finite Element Hybrid (SIFEH) Method for Fracture Mechanics," International Journal for Numerical Methods in Engineering, Vol. 20, pp. 869-885, 1984.

19. Annigeri, B. S. and Cleary, M. P.: "Quasi-Static Crack Propagation Using the Surface Integral Finite Element Hybrid Method," ASME Pressure Vessels and Piping Conference, ASME PVP-85, San Antonio, Texas, June 1984.

20. Annigeri, B. S.: "Effective Modeling of Stationary and Propagating Cracks using the Surface Integral and Finite Element Hybrid Method," ASME Winter Annual Meeting, Miami, November 1985, ASME AMD Vol. 72, 1985.

21. Annigeri, B. S.: "Fracture Mechanics Analysis for Short Cracks," Annual Report, UTRC Report No. R87-957565-1, Prepared for the Air Force Office of Scientific Research, Contract No. F49620-86-C-0095, August 1987.

22. Keat, W. D.and Cleary, M. P.: "Development of a Surface Integral and Finite Element Hybrid Capability for the Analysis of Fractures in Three Dimensional Bounded Continua," MIT UFRAC Report No. REL-84-6, September 1984.

23. Keat, W. D., Annigeri, B. S. and Cleary, M. P.: "Surface Integral and Finite Element Hybrid Method for Two and Three Dimensional Fracture Mechanics Analysis," International Journal of Fracture, Vol. 36, pp. 35-53, 1988.

24. Rice, J. R.: in "Mechanics of Crack Tip Deformation and Extension by Fatigue," ASTM STP 415, pp. 247-311, 1967.

25. Vitek, V.: "Yielding on Inclined Planes at the Tip of a Crack Loaded in Uniform Tension," Journal of the Mechanics and Physics of Solids, Vol. 24, pp. 263-275, 1976.

26. Lo, K. K.: "Modeling of Plastic Yielding at a Crack Tip by Inclined Slip Planes," International Journal of Fracture, Vol. 15, pp. 583-589, 1979.

27. Riedel, H.: "Plastic Yielding on Inclined Slip-Planes at a Crack Tip," Journal of the Mechanics and Physics of Solids, Vol. 24, pp. 277-289, 1976.

28. Gu, I.: "Medium-Scale Yielding Analysis of an Angled Crack and Slipline Analysis of the Crack-Hole Interaction," Ph.D. Thesis, Department of Mechanical Engineering, MIT, 1982.

29. Budiansky, B. and Hutchinson, J. W.: "Analysis of Closure in Fatigue Crack Growth," Journal of Applied Mechanics, Vol. 45, pp. 267-276, 1978.

30. Hellan, K.: Introduction to Fracture Mechanics, McGraw-Hill Book Co., 1984.

31. Carnahan, B., Luther, H. A., and Wilkes, J. O.: "Applied Numerical Methods", John Wiley, New York, 1969.

32. Annigeri, B. S.: "Fracture Mechanics Analysis for Short Cracks," Annual Report, UTRC Report No. R88-957565-2, Prepared for the Air Force Office of Scientific Research, Contract No. F49620-86-C-0095, August, 1988.

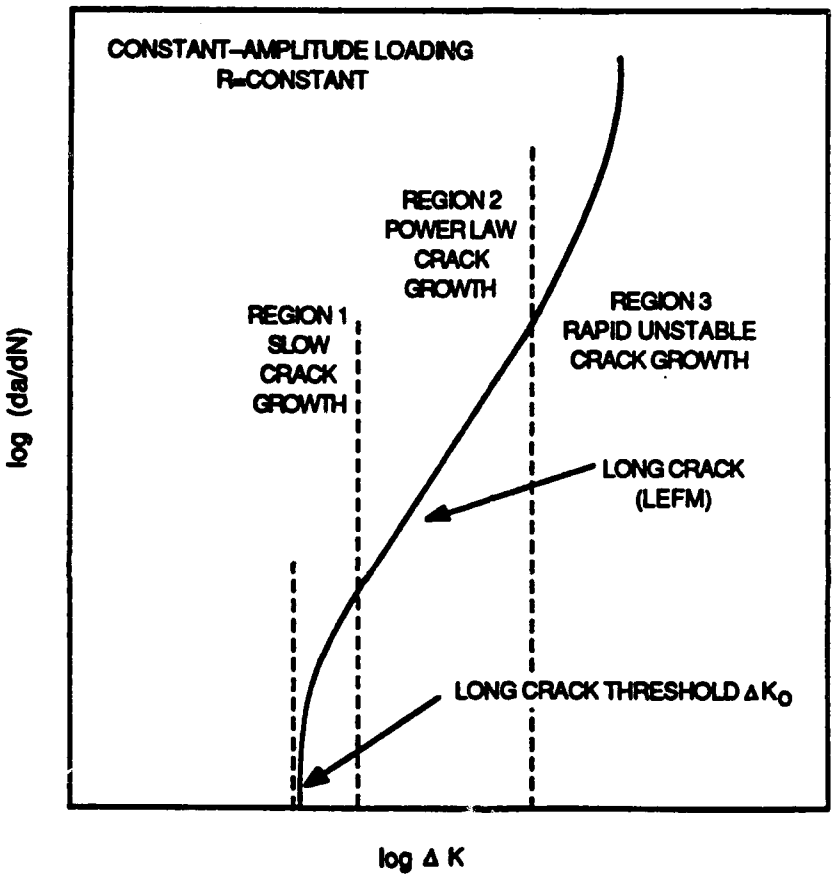

Figure 1. The different regimes of fatigue crack growth (typical long crack data).

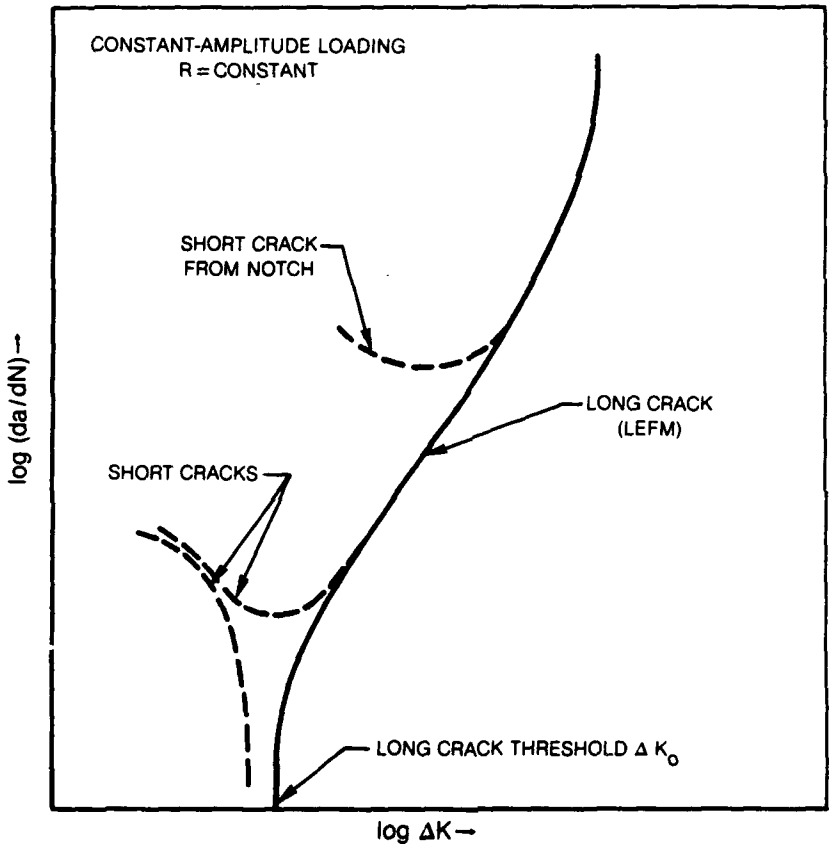

Figure 2. Typical fatigue crack propagation rates (da/dN) for long and short cracks as function of stress intensity factor range ΔK [Ref. 10].

86-2-1-1

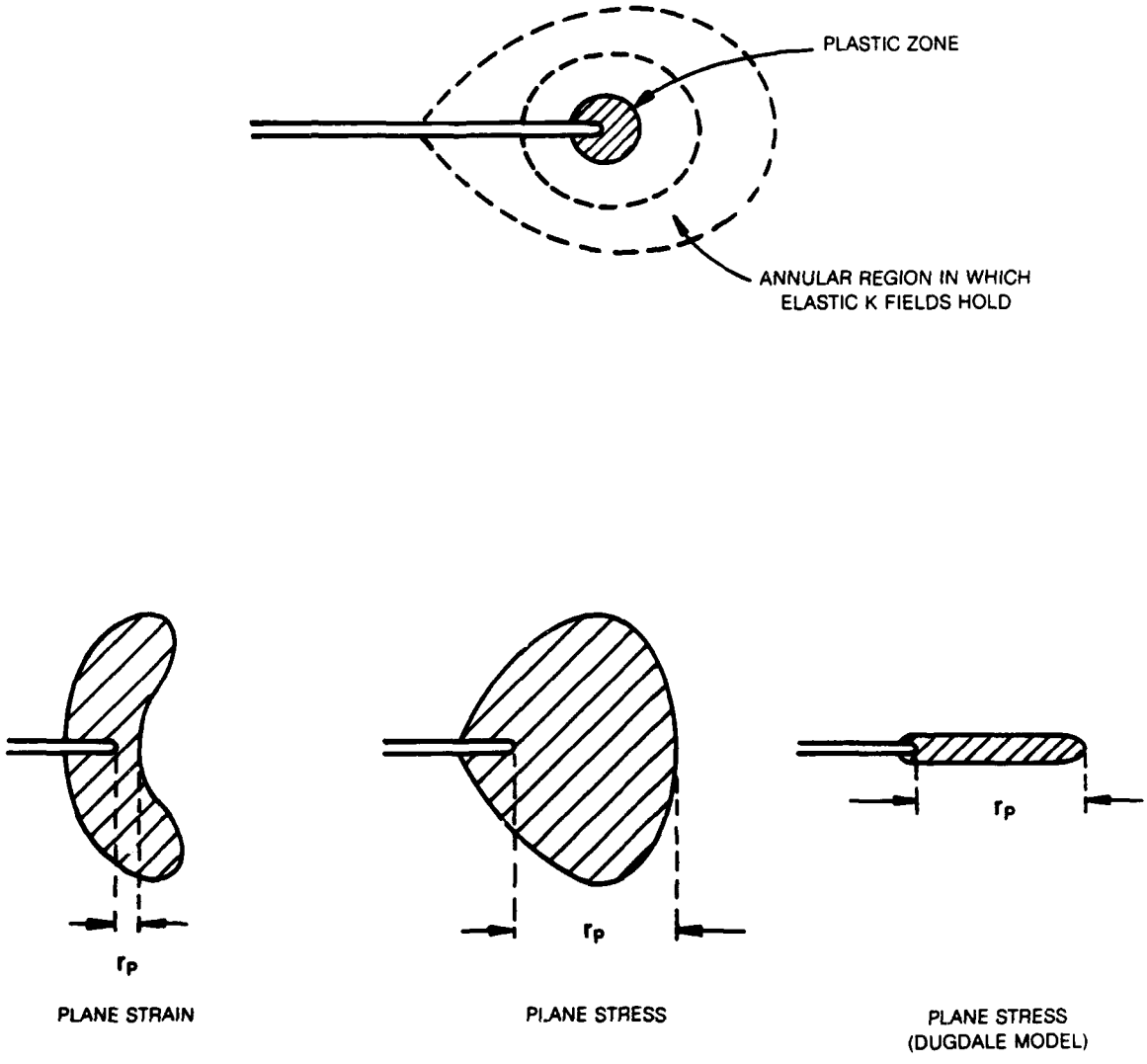

Figure 3. Crack tip plastic zones for various conditions. (Monotonic loading)

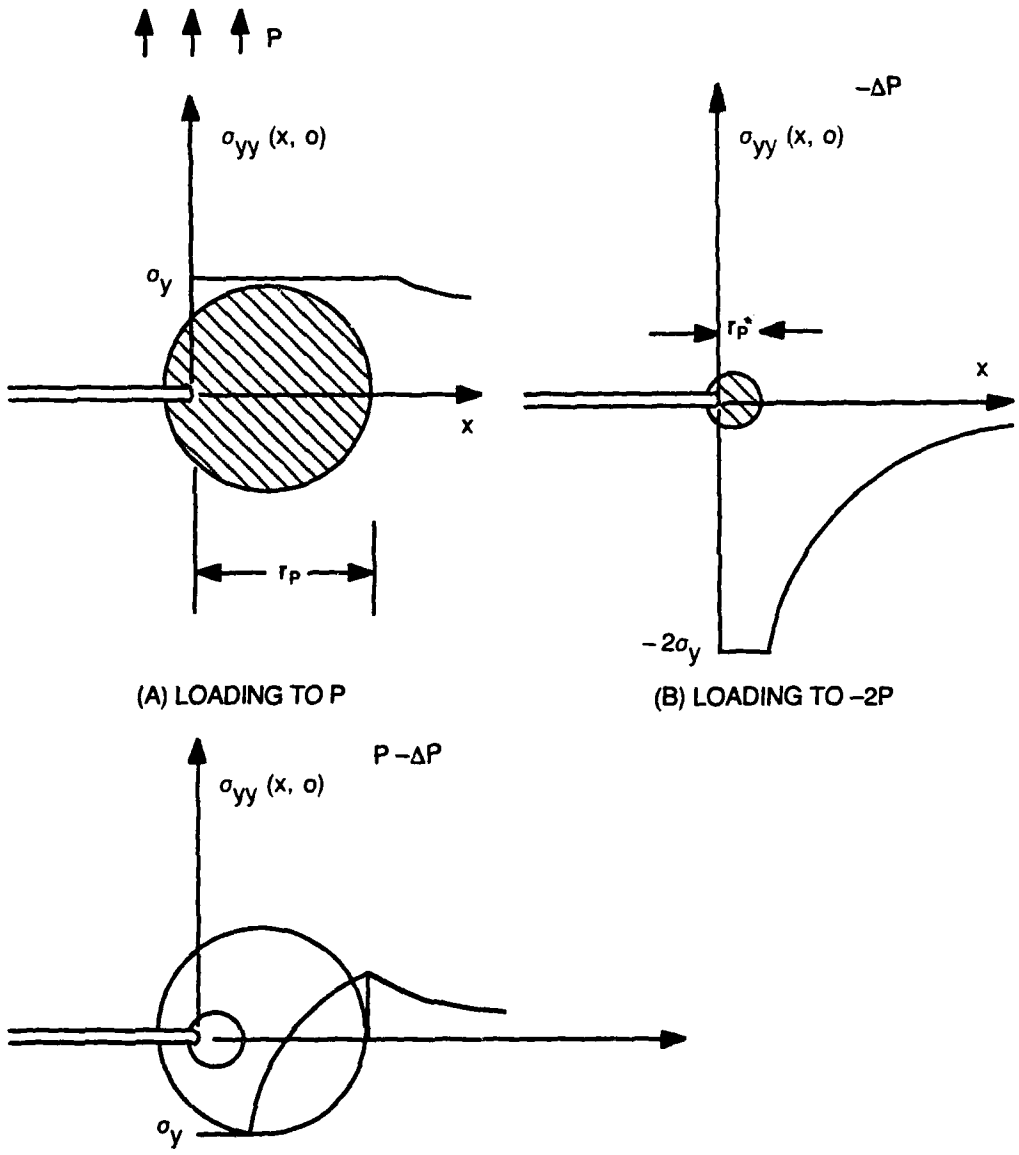

Figure 4. Mode I plastic zone size for elastic-perfectly plastic flow and proportional loading (24).

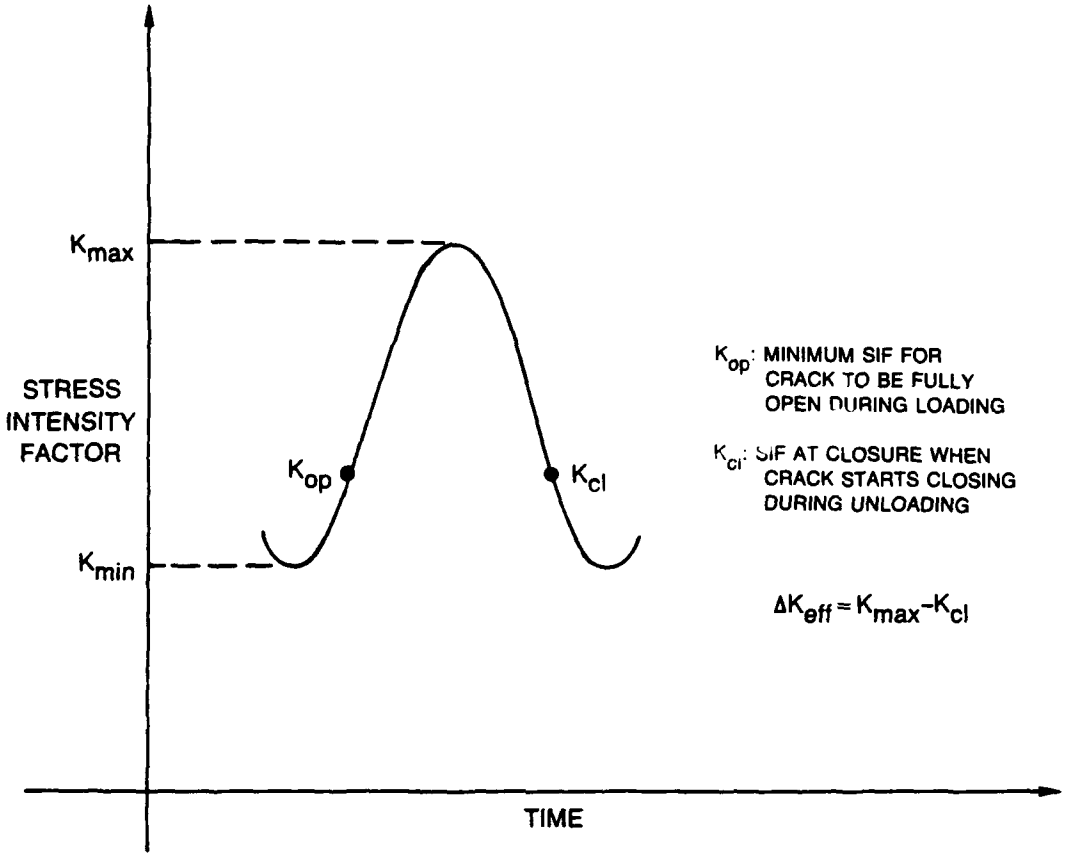

Figure 5. Opening and closure stress intensity factors during fatigue crack propagation [16].

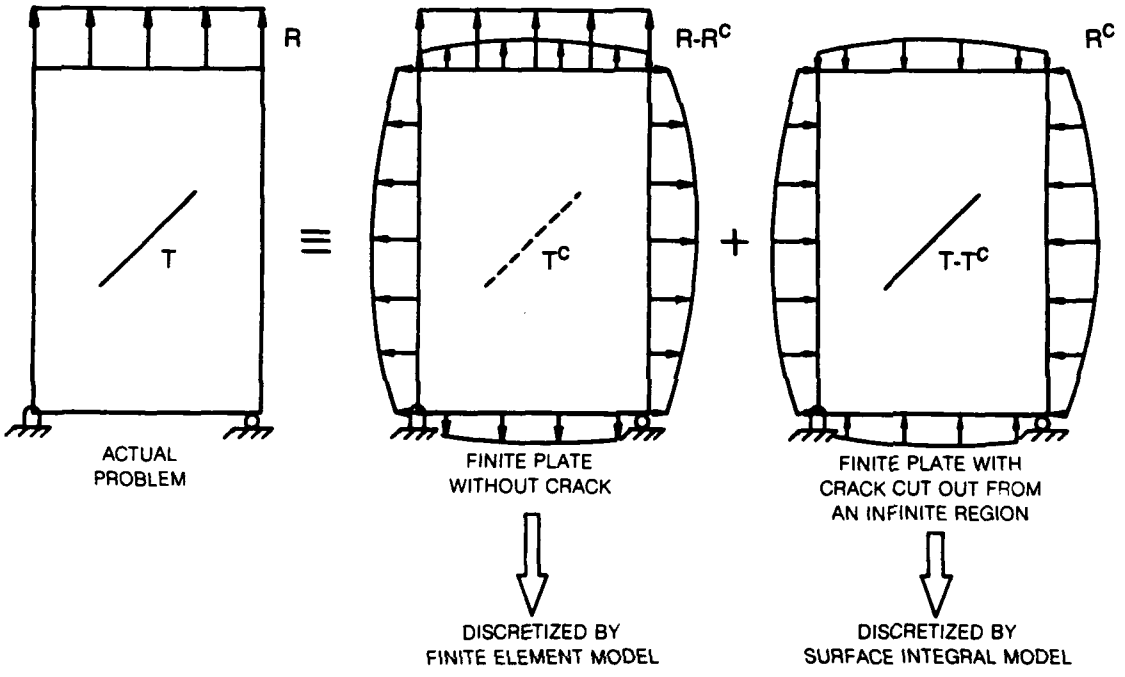

Figure 6. Linear superposition of the finite element and surface integral models.

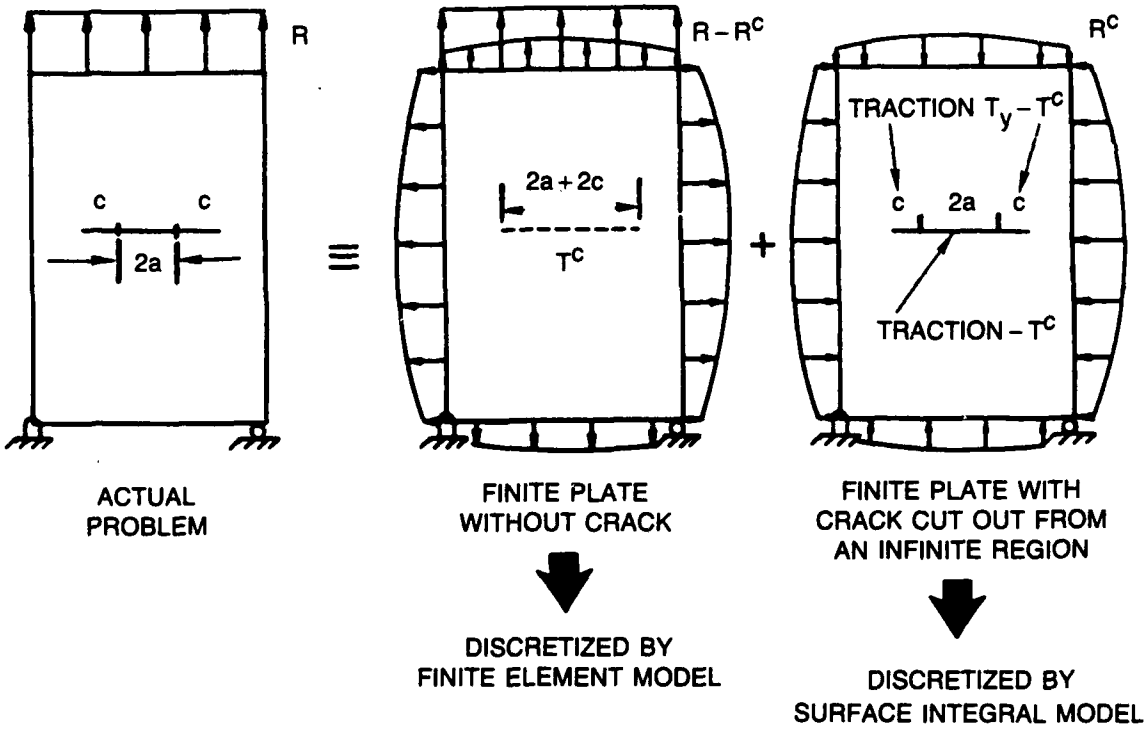

Figure 7. Superposition of the surface integral and finite element models including yield strips.

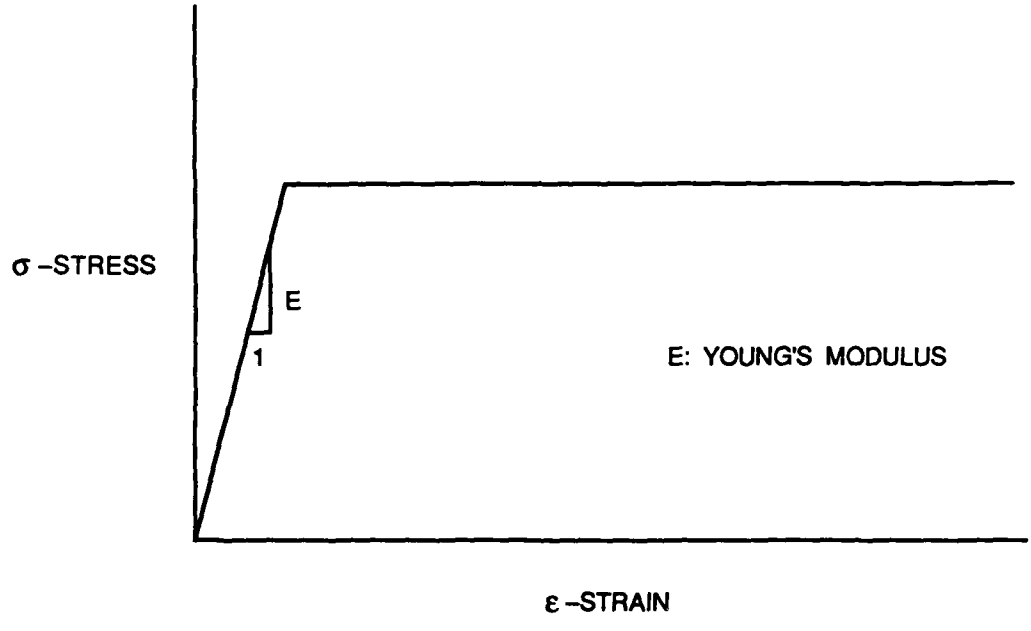

Figure 8. Elastic–Perfectly Plastic Material Model.

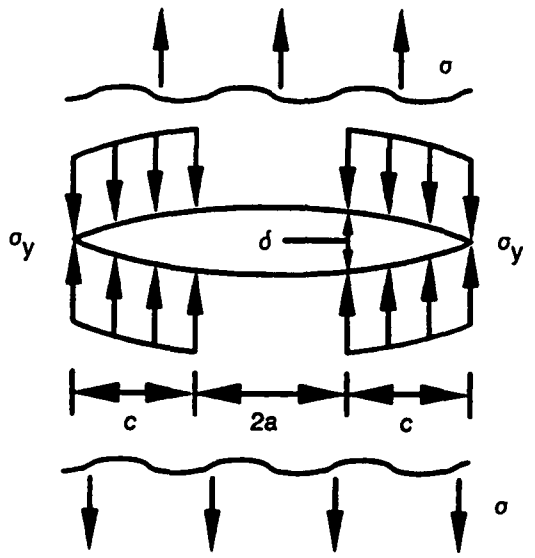

CRACK TIP OPENING
SHOWN IN DETAIL

$$\delta_{DUGDALE} = \frac{8}{\pi} \frac{\sigma_y}{E} a \ln \left[\sec \left(\frac{\pi}{2} \frac{\sigma}{\sigma_y}\right)\right]$$

$$c_{DUGDALE} = a \left[\sec \left(\frac{\pi}{2} \frac{\sigma}{\sigma_y}\right) - 1\right]$$

Figure 9. Dugdale yield strip model.

88-8-35-6

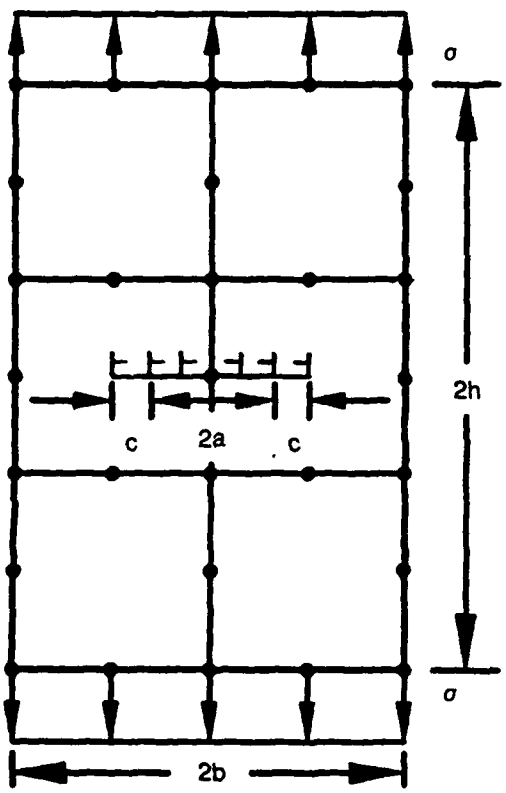

2a CRACK LENGTH

c YIELD STRIP LENGTH
(OBTAINED BY ITERATION))

2h = 12	$\sigma_y = 30{,}000$ psi
2b = 4	$\sigma = 15{,}000$ psi
	$E = 3.\ 10^7$ psi

┤ REPRESENTS OPENING DISLOCATION

Figure 10. Hybrid model for center cracked panel under tensile loading.

88—8—35—7

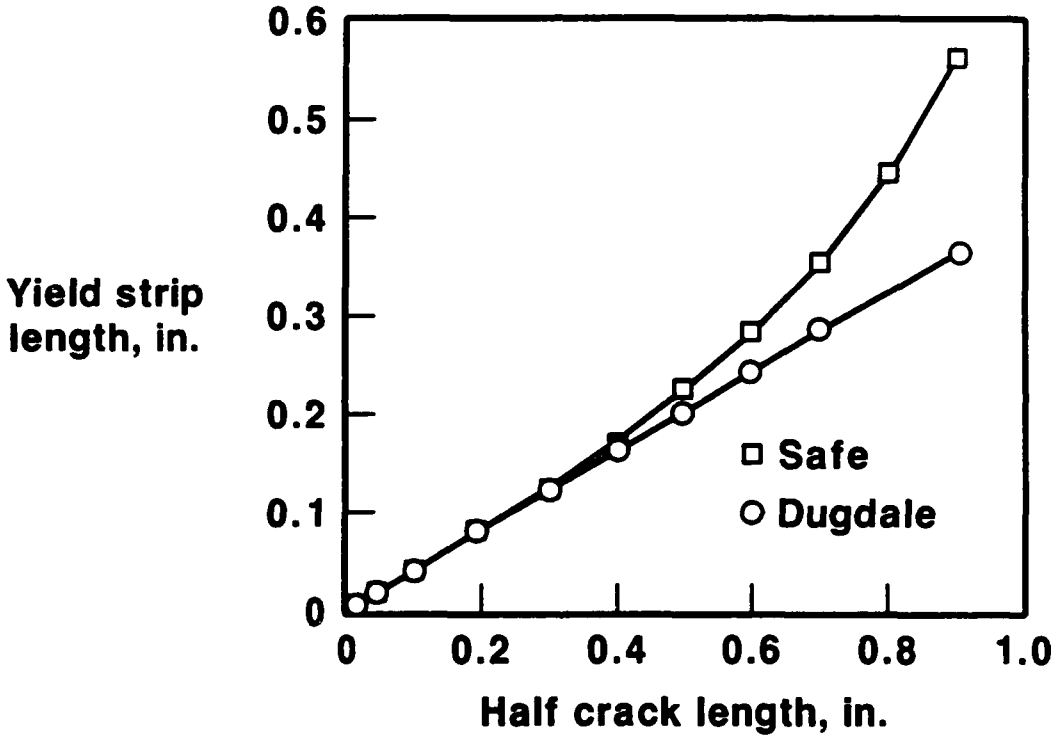

Figure 11. Yield strip lengths for mode I loading.

90-2-48-4

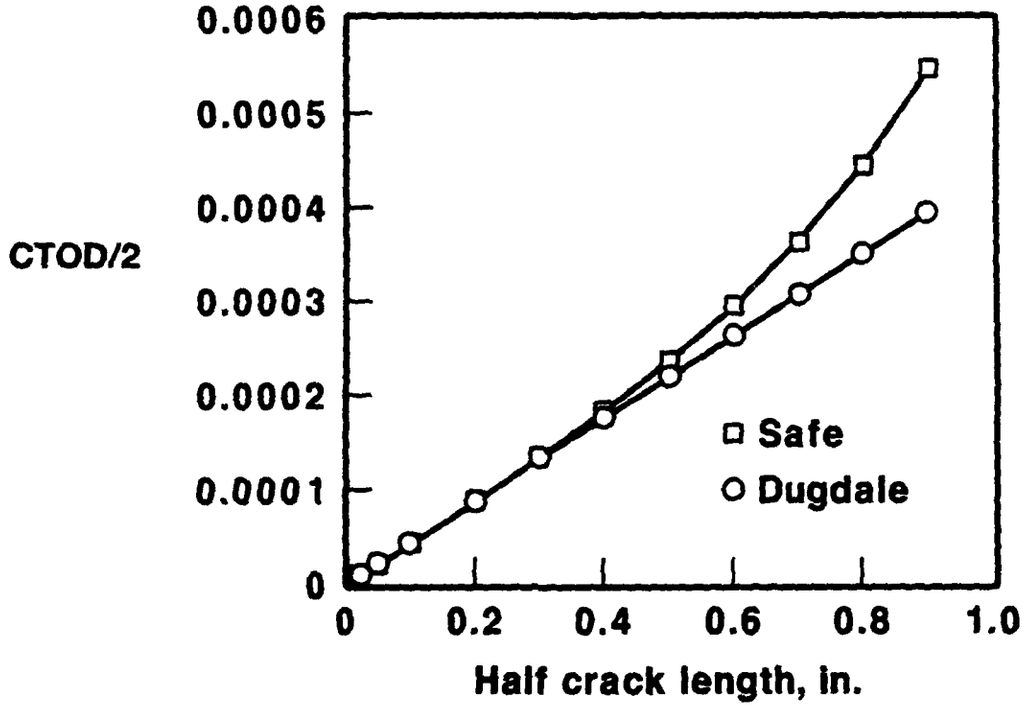

Figure 12. Crack tip opening displacement (CTOD) for mode I loading.

90-2-48-5

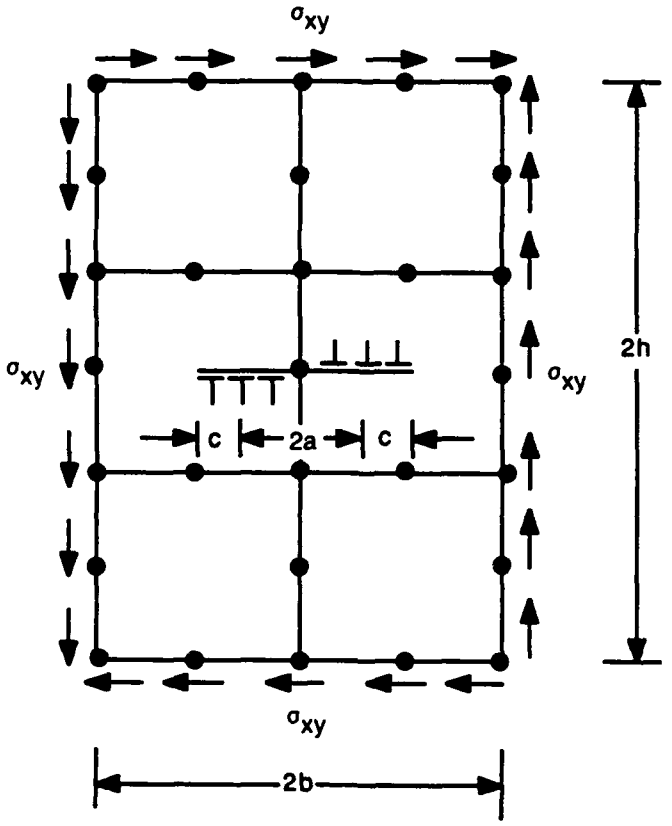

2a CRACK LENGTH

c YIELD STRIP LENGTH
(OBTAINED BY ITERATION)

2h = 12 σ_y = 30,000 psi
2b = 4 σ_{xy} = 15,000 psi
E = 3. 10^7 psi

⊥ REPRESENTS SLIP DISLOCATION

Figure 13. Hybrid model for center cracked panel under shear loading.

88—8—35—8

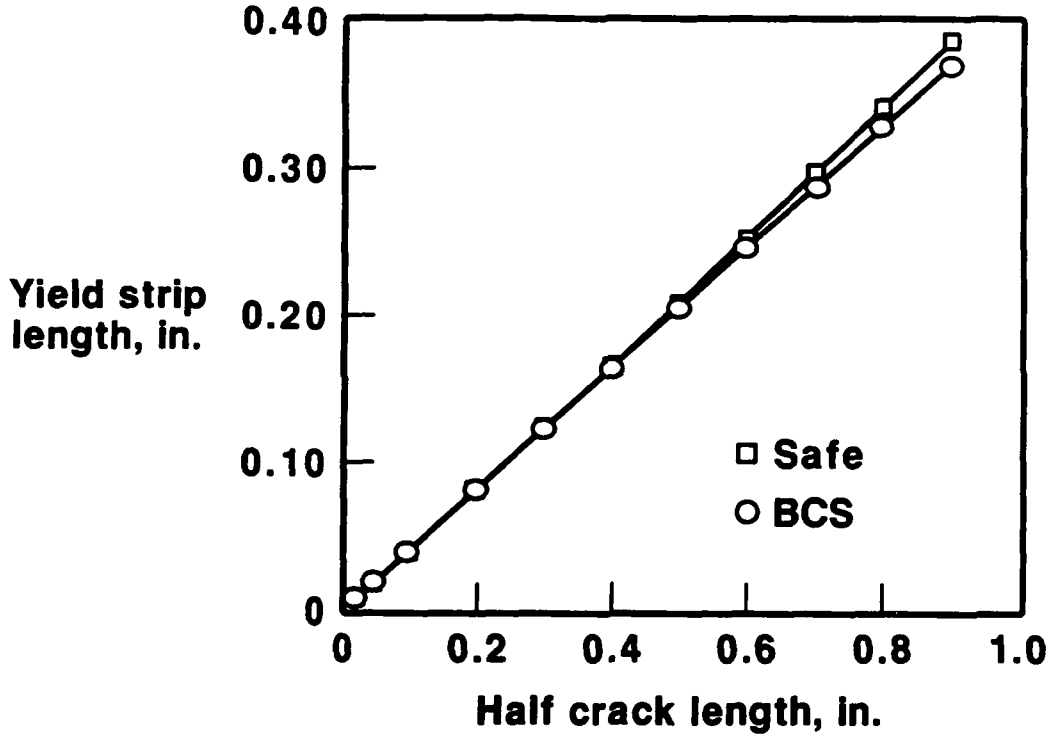

Figure 14. Yield strip lengths for mode II loading.

90-2-48-6

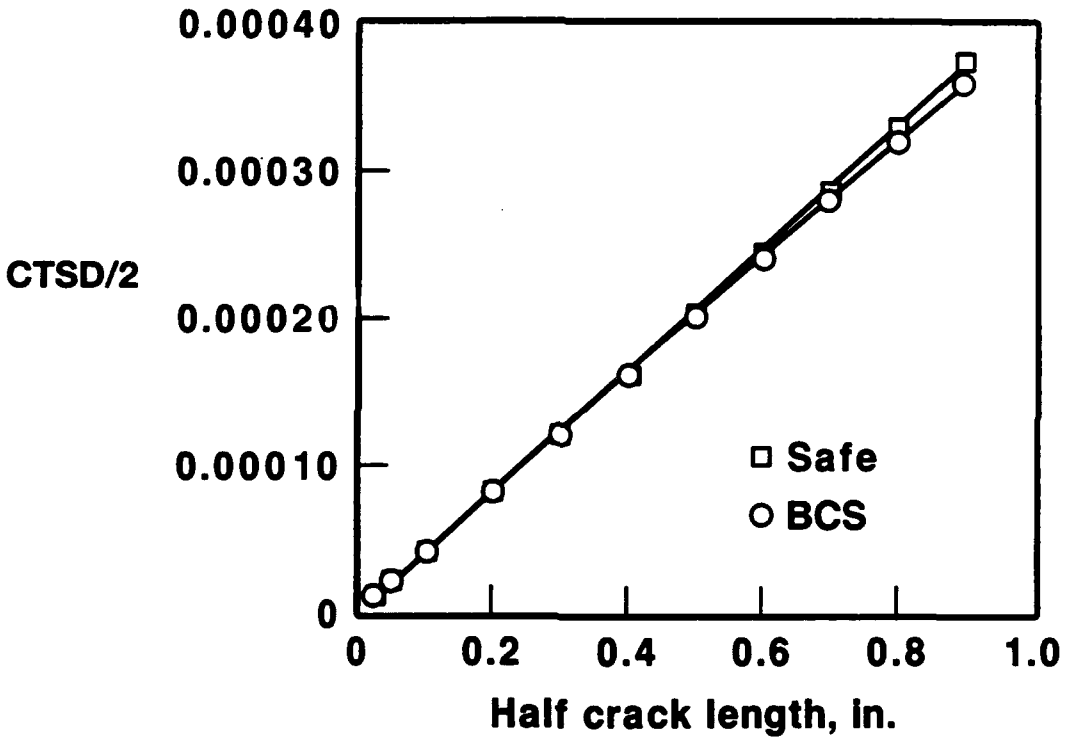

Figure 15. Crack tip slip displacement (CTSD) for mode II loading.

90-2-48-7

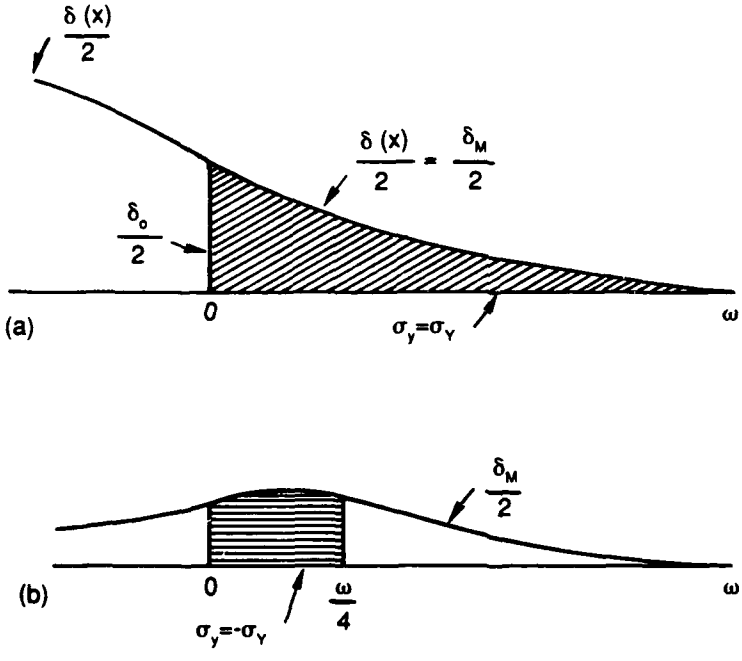

Figure 16. Dugdale model, stationary crack: (a) $K=K_{max}$ and (b) unloading to K=0 (Ref. 29).

90-2-48-2

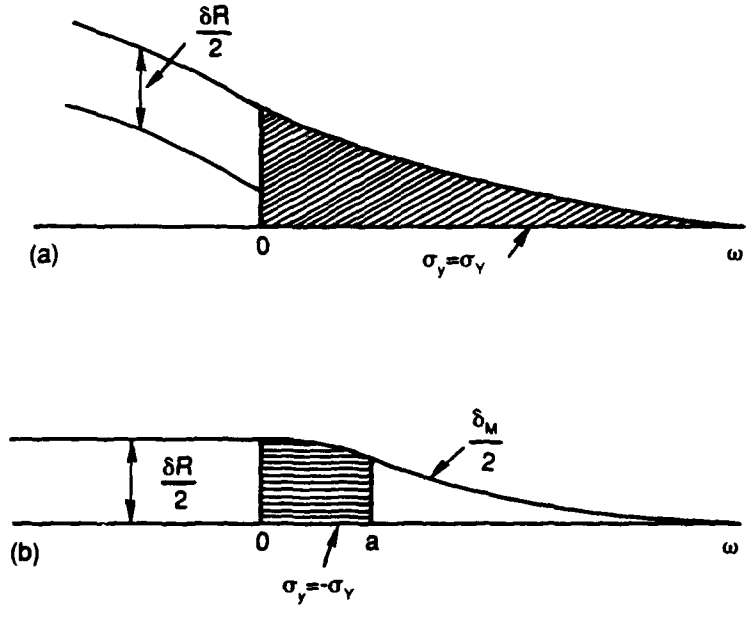

Figure 17. Growing crack: (a) $K=K_{max}$ and (b) $K=K_{min}=0$ (Ref. 29).

90-2-48-3

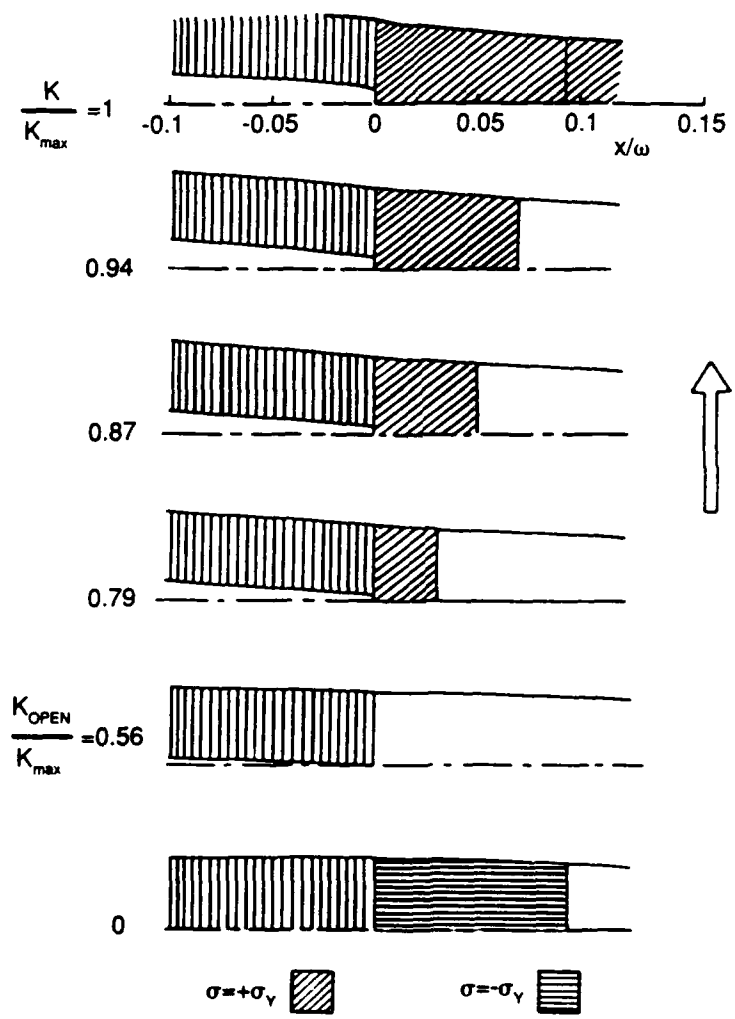

Figure 18. Crack opening process ($K=0 \rightarrow K=K_{max}$) (Ref. 29).

90-2-48-1

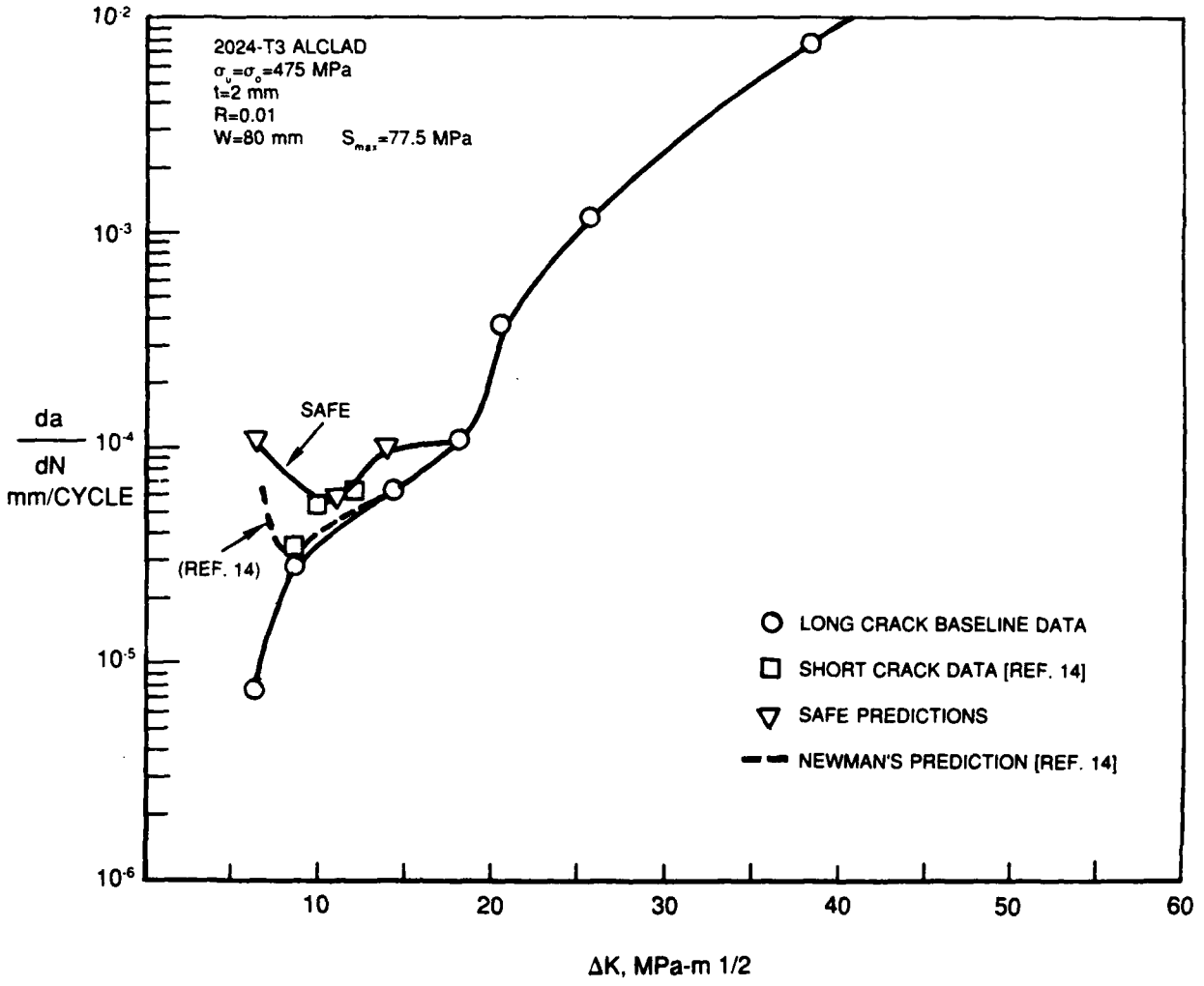

Figure 19 Experimental and predicted crack growth rates for small cracks.

90-2-48-8